Supplementary Information

Tuning the Chemical Environment of Palladium Bimetallic Nanocatalysts via C_3N_4 Support Engineering and Bimetallic Synergy for Boosted Visible-Light-Driven Hydrogen Evolution from Formic Acid

Zhichao Feng, †[a,b] Hao Zhang, †[a,b] Mingyao Hou, [b] Bo Hai [b] and Lijun Ding *[a,b]

[a] National Forestry Grassland Engineering Technology Research Center for Efficient Development and Utilization of Sandy Shrubs Give contact information, Department of Chemistry and Chemical Engineering, College of Science, Inner Mongolia Agricultural University, Hohhot, Inner Mongolia 010018, China.

[b] College of Science, Inner Mongolia Agricultural University, Hohhot, Inner Mongolia 010018, China.

† These authors contributed to the work equally and should be regarded as co-first authors.

* Corresponding author.

E-mail addresses: dlj78@163.com

KEYWORDS: hydrogen evolution, metal nanoparticle, semiconductor, catalyst, visible light irradiation

Table of contents

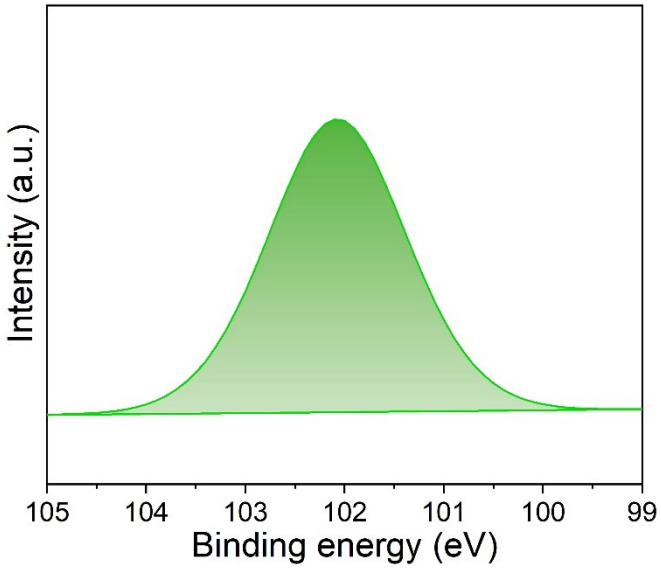

Figure S1. High-resolution Si 2p XPS spectra of PdNi/CNU.

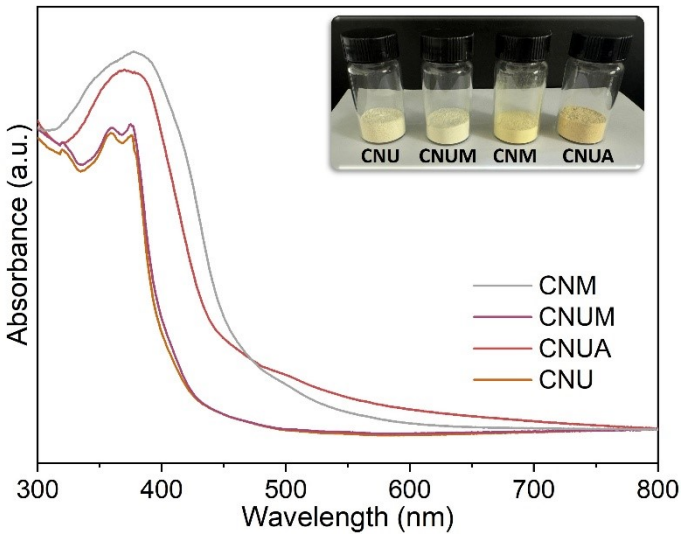

Figure S2. UV–vis DRS spectra of CNU, CNUA, CNUM and CNM.

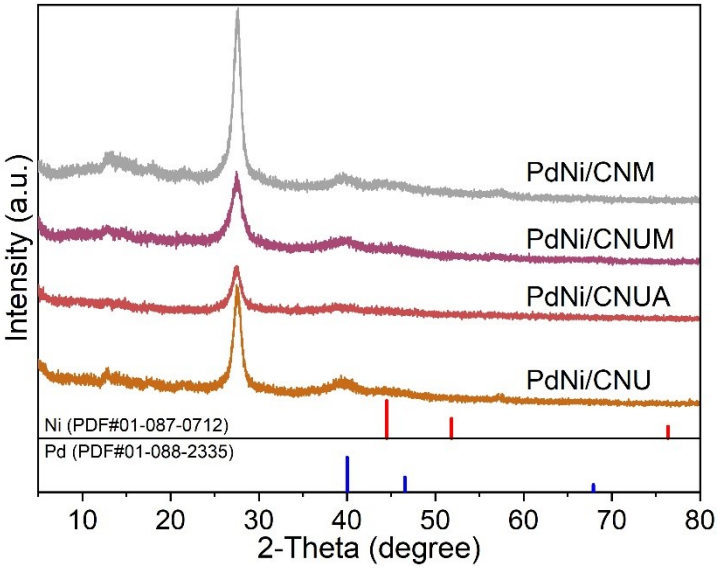

Figure S3. PXRD patterns of PdNi/CNU, PdNi/CNUA, PdNi/CNUM and PdNi/CNM.

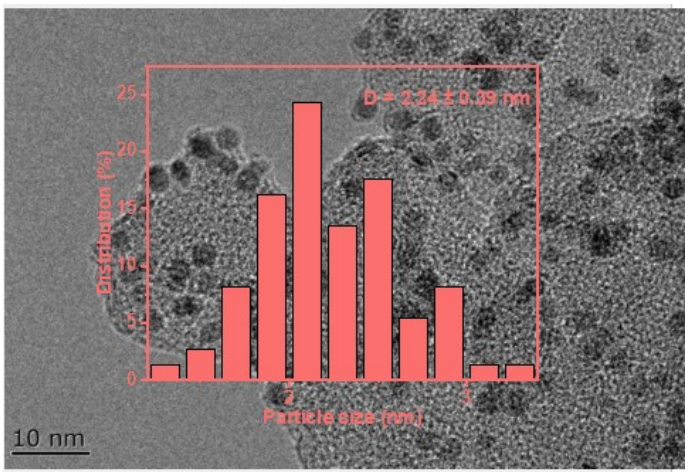

Figure S4. A representative TEM image of PdNi/CNUM, showing the morphology and size uniformity of PdNi NPs (inset, particle size distribution of PdNi NPs).

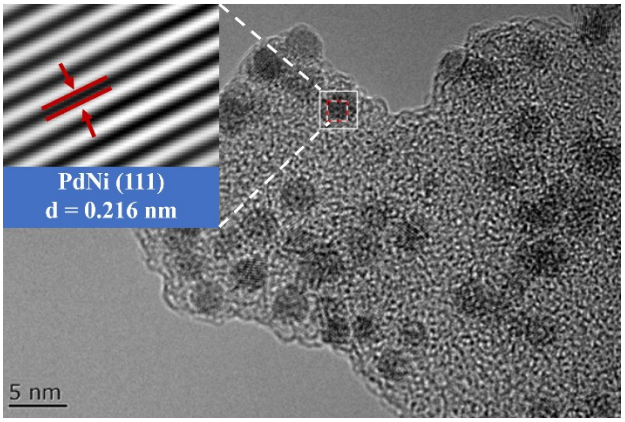

Figure S5. HRTEM and enlarged HRTEM image of PdNi/CNUM.

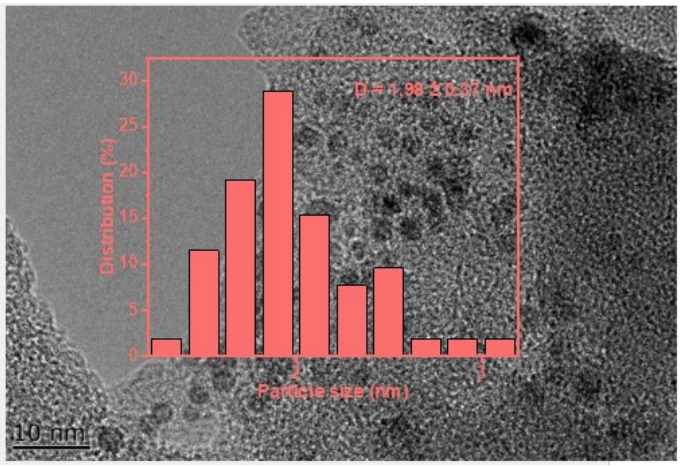

Figure S6. A representative TEM image of PdNi/CNM, showing the morphology and size uniformity of PdNi NPs (inset, particle size distribution of PdNi NPs).

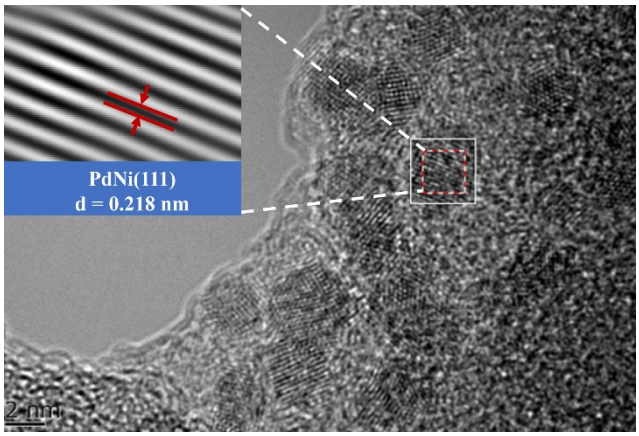

Figure S7. HRTEM and enlarged HRTEM image of PdNi/CNM.

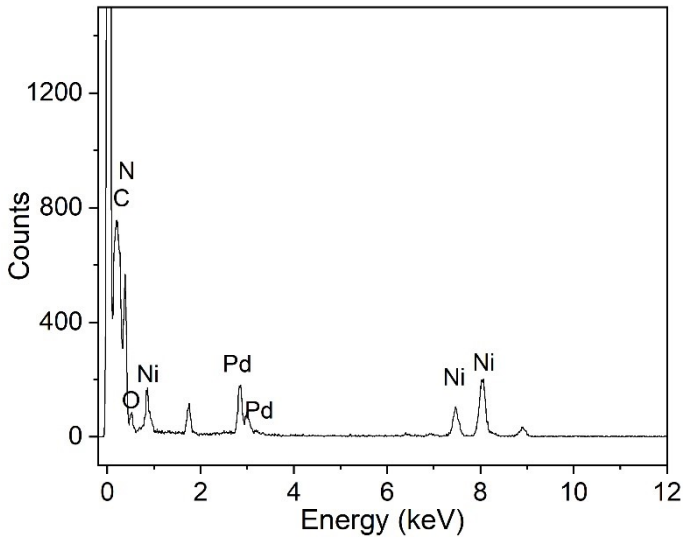

Figure S8. EDX pattern of PdNi/CNU.

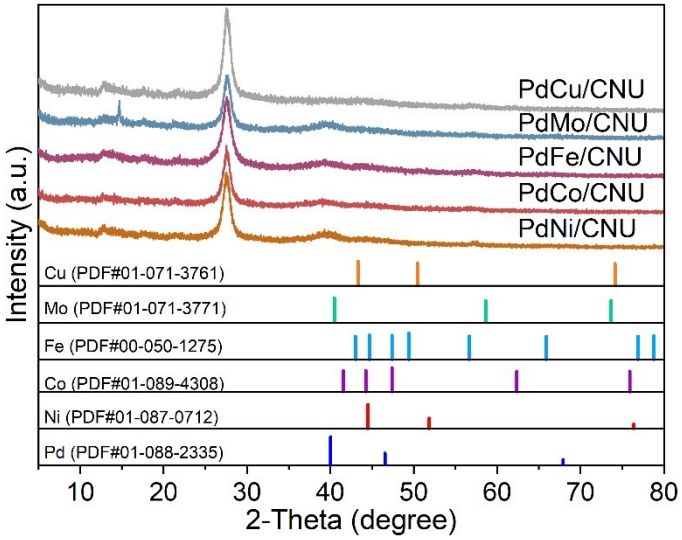

Figure S9. PXRD patterns of bimetallic Pd-based nanocatalysts.

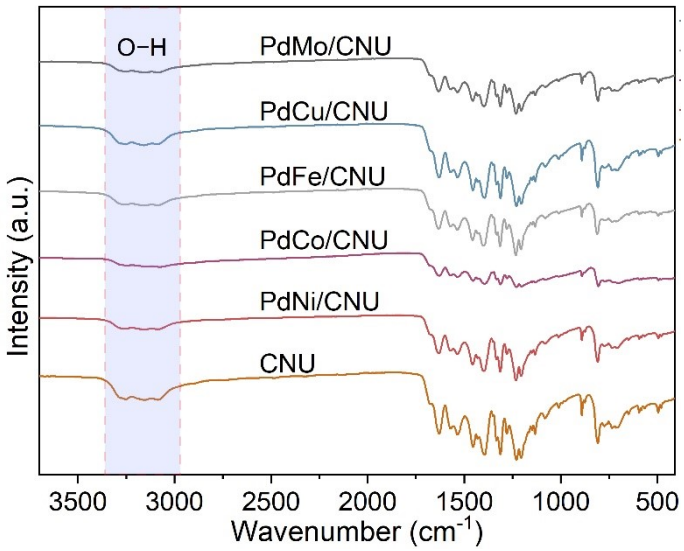

Figure S10. IR spectra of CNU and bimetallic Pd-based nanocatalysts.

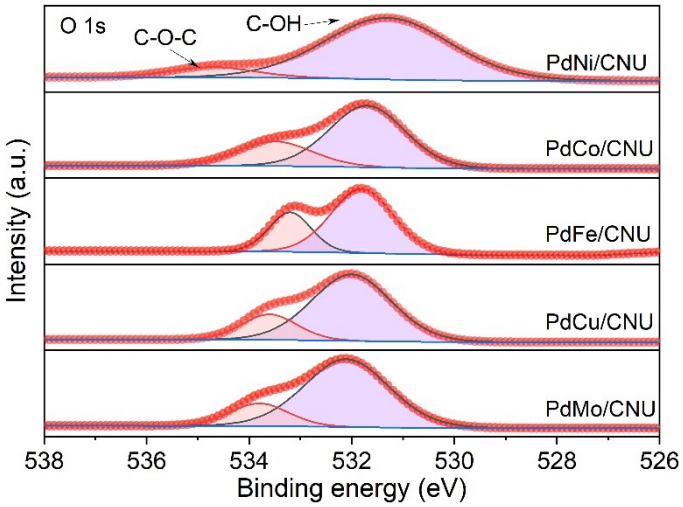

Figure S11. High-resolution O 1s XPS spectra of bimetallic Pd-based nanocatalysts.

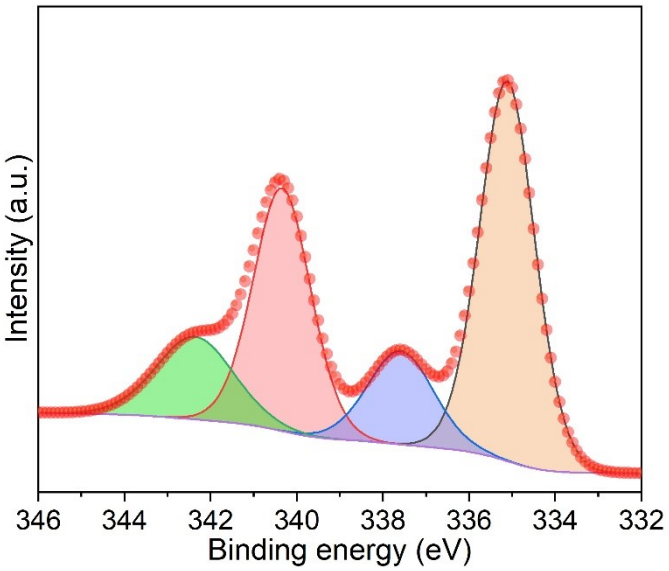

Figure S12. High-resolution Pd 3d XPS spectra of Pd/CNU.

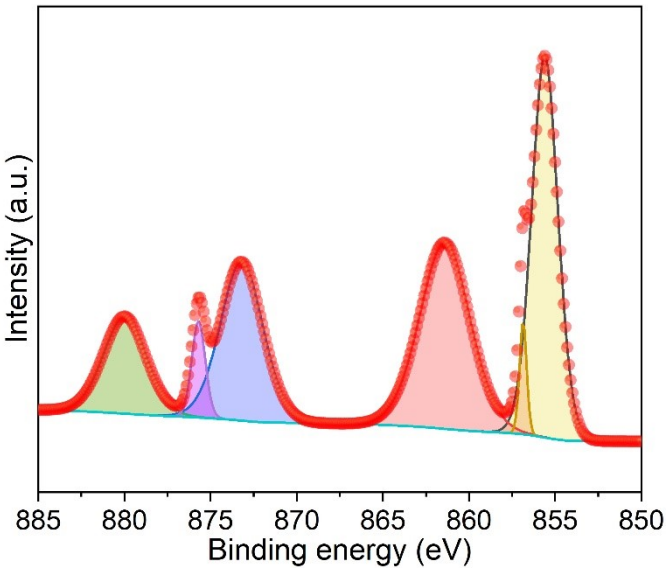

Figure S13. High-resolution Ni 2p XPS spectra of PdNi/CNU.

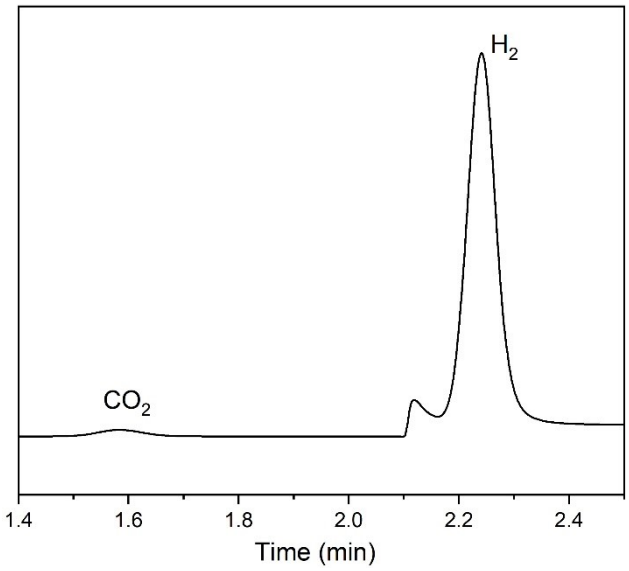

Figure S14. GC spectra obtained using TCD for the evolved gas from HCOOH aqueous solution over PdNi/CNU under visible light irradiation.

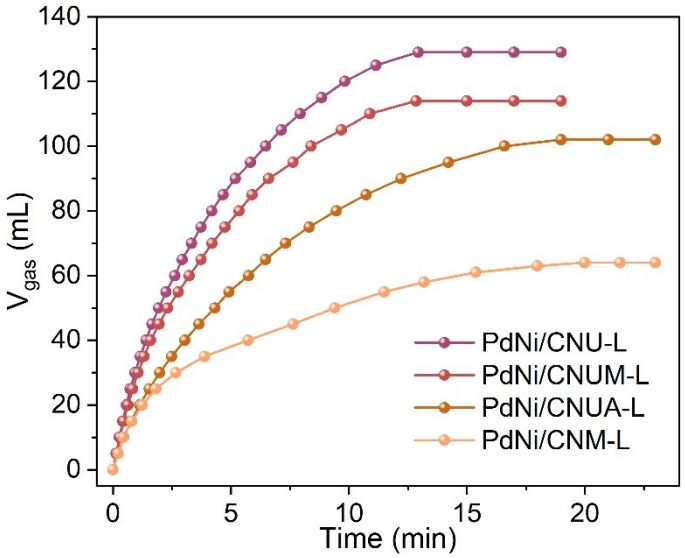

Figure S15. Plots of time *versus* volume of generated H_2 from HCOOH over PdNi/CNU, PdNi/CNUA, PdNi/CNUM and PdNi/CNM under visible light irradiation.

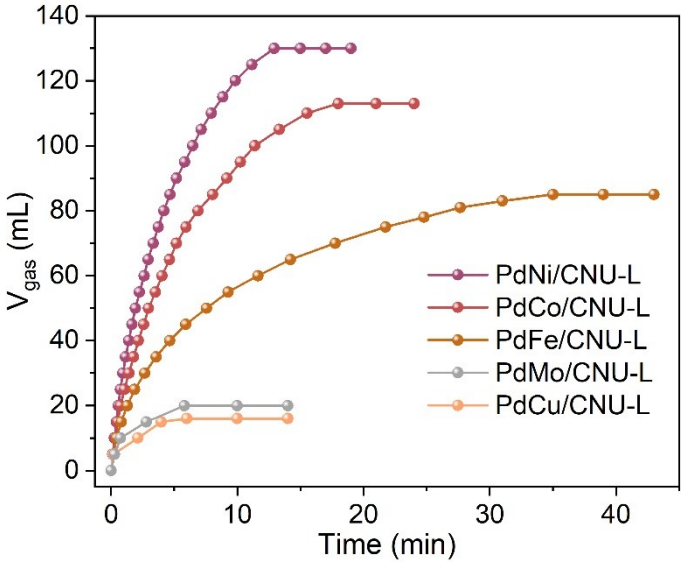

Figure S16. Plots of time *versus* volume of generated H_2 from HCOOH over CNU-supported Pd-based bimetallic catalysts with different second metal components under visible light irradiation.

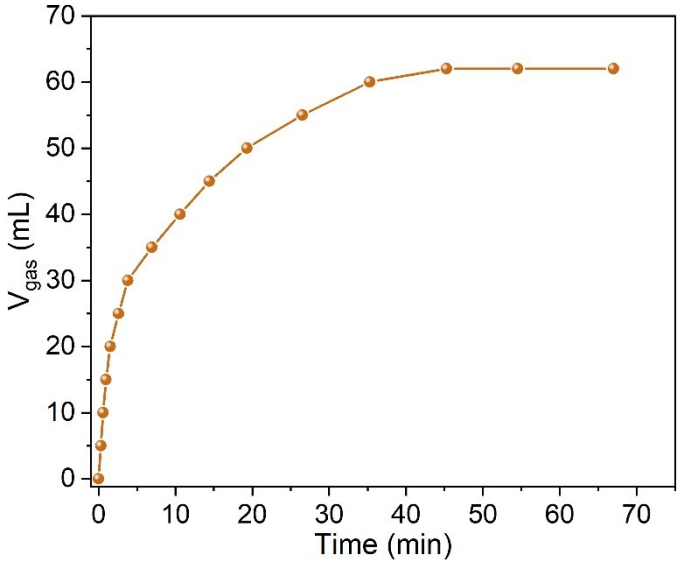

Figure S17. Plots of time *versus* volume of generated H_2 from HCOOH over Pd/CNU under visible light irradiation.

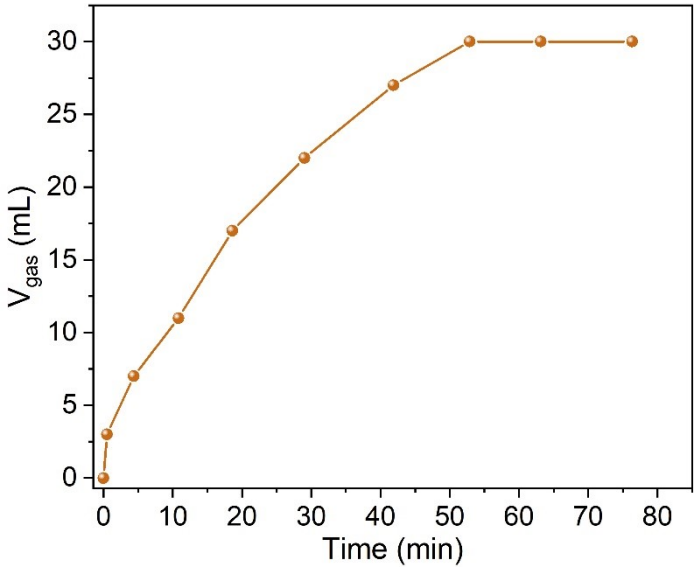

Figure S18. Plots of time *versus* volume of generated H_2 from HCOOH over PdNi/CNU-0APTES under visible light irradiation.

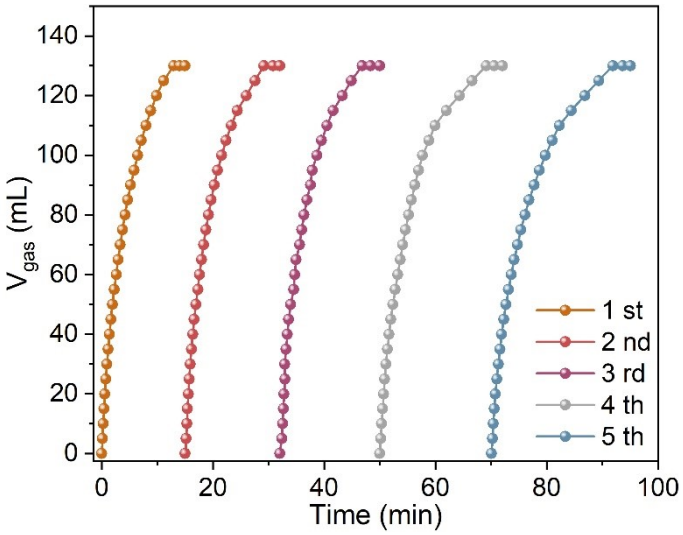

Figure S19. Long-time durability test for generated H_2 from HCOOH aqueous solution over PdNi/CNU under visible light irradiation at 298 K.

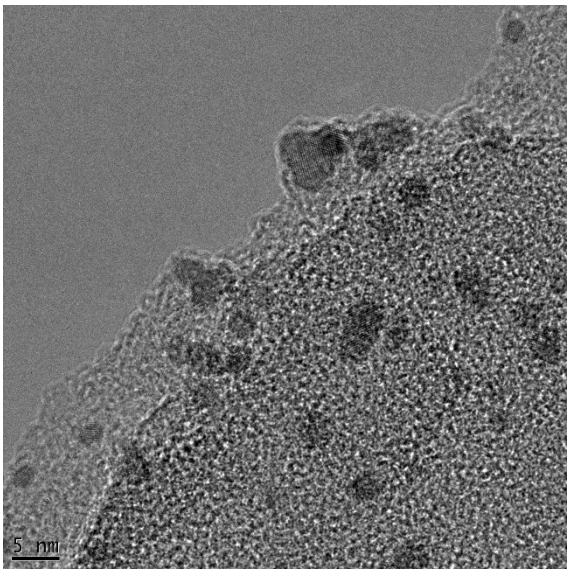

Figure S20. HRTEM image of PdNi/CNU after reaction.

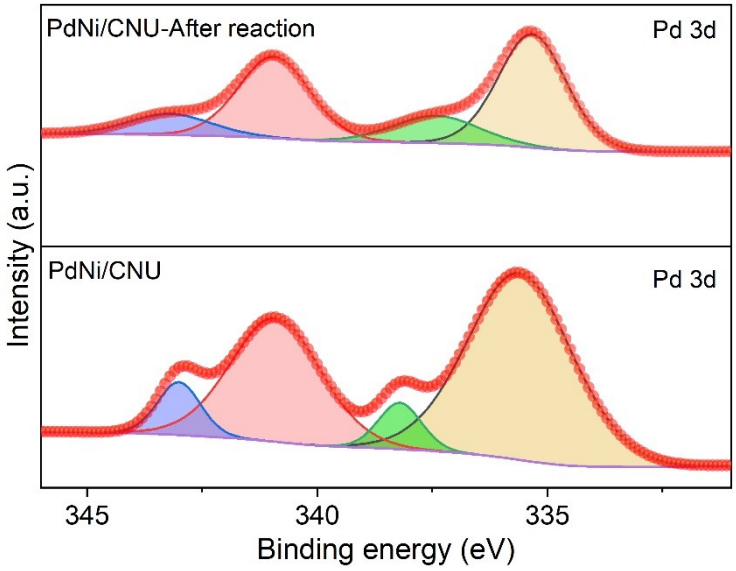

Figure S21. High-resolution Pd 3d XPS spectra of PdNi/CNU before and after reaction.

Table S1. Metal Loadings in catalysts measured by ICP-MS.

Samples	Pd (wt.%)
PdNi/CNU	3.94
PdNi/CNU (After reaction)	3.52
PdNi/CNUM	3.83
PdNi/CNUA	4.04
PdNi/CNM	3.93
PdCo/CNU	3.84
PdFe/CNU	3.92
PdCu/CNU	3.99
PdMo/CNU	3.97
Pd/CNU	3.63

Table S2. Activities of catalysts in hydrogen generation from hydrolysis of HCOOH.

Catalysts	TOF (h^{-1})	Reference
PdNi/CNU	751.8	This work
Au@GO-SiO2	539	1
Pd–Ni–Ag/C	85	2
1 : 3 PdCo	324.6	3
$Au_{0.28}Pd_{0.47}Co_{0.25}$/MIL-101$NH_2$	347	4
$Au_1Pd_{1.5}$/MIL-101-NH_2	526	5
AgPd@MIL-100(Fe)	58	6
PdAg/SBA-15-Amine	65	7
$Co_{48}Au_5Pd_{47}$@ MIL-101-NH_2	60	8
AuPd–MnOx/MoF–rGO	382	9
PdRu/C_3N_4 5%	95.24	10

References

1 S. Mousavi-Salehi, S. Keshipour and F. Ahour, *J. Phys. Chem. Solids*, 2023, **176**, 111239.

2 M. Yurderi, A. Bulut, M. Zahmakiran, and M. Kaya, *Appl. Catal., B*, 2014, **160**−**161**, 514−524.

3 M. Ribota Peláez, E. Ruiz-Lopez, M. I. Dominguez, S. Ivanova, and M. A. Centeno, *Catalysts*, 2023, **13**, 977.

4 J. Cheng, X. Gu, P. Liu, T. Wang and H. Su, *J. Mater. Chem. A*, 2016, **4**, 16645−16652.

5 J. Cheng, X. Gu, P. Liu, H. Zhang, L. Ma and H. Su, *Appl. Catal. B: Environ.*, 2017, **218**, 460−469.

6 F. Ke, L. Wang, J. Zhu, *Nanoscale*, 2015, **7**, 8321−8325.

7 K. Mori, Y. Futamura, S. Masuda, H. Kobayashi and H. Yamashita, *Nat. Commun.*, 2019, **10**, 4094.

8 P. Zhao, W. Xu, D. Yang, W. Luo and G. Cheng, *ChemistrySelect*, 2016, **1**, 1400−1404.

9 J.-M. Yan, Z.-L. Wang, L. Gu, S.-J. Li, H.-L. Wang, W.-T. Zheng and Q. Jiang, *Adv. Energy Mater.*, 2015, **5**, 1500107.

10 E. Ruiz-López, M. Ribota Peláez, M. BlascoRuz, M. I. Domínguez Leal, M. Martínez Tejada, S. Ivanova and M. Á. Centeno, *Materials*, 2023, **16**, 472.